Interaction between vortices and compliant walls

Alessandro Bottaro
DICAT, Università di Genova

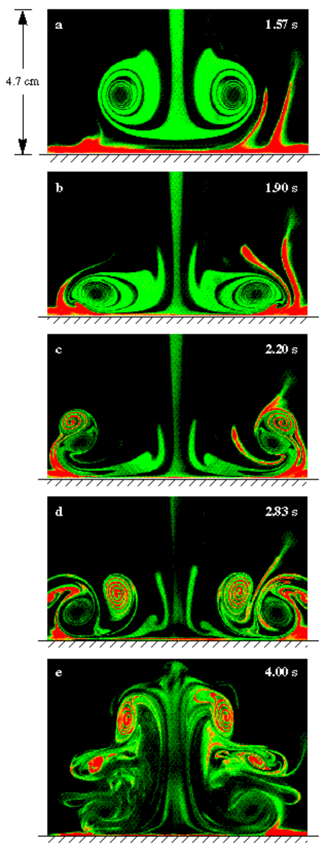

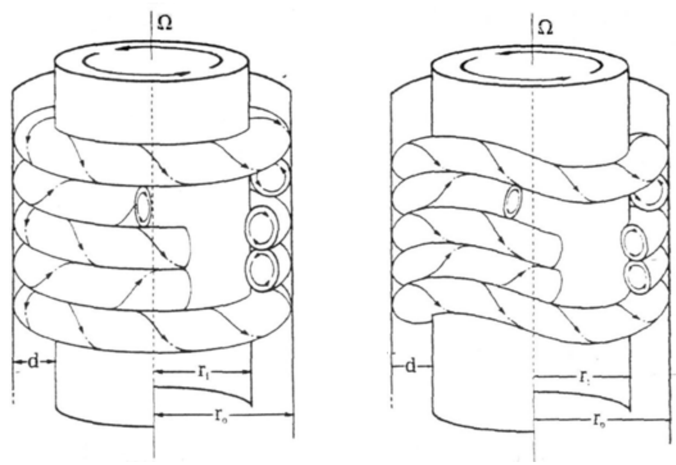

Taylor vortices and wavy Taylor vortices

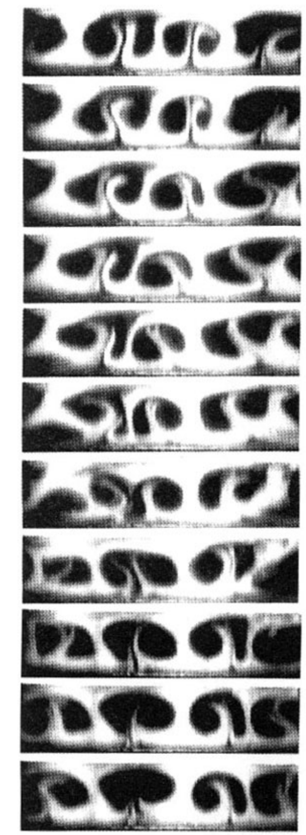

C. P. Gendrich, M. M. Koochesfahani, and D. G. Nocera (1997)
Molecular Tagging Velocimetry and Other Novel Applications of a New Phosphorescent Supramolecule. *Experiments in Fluids*, **23**(5): 361-72.

Smoke flow visualization by
Phil Ligrani, University of Utah

OUTLINE

- Significance of the subject
- Previous work on linear stability of flows over compliant walls
- Dean and Taylor vortex flows: the fluid model
- Shell theory: the wall model
- Linear stability: hydroelastic and hydrodynamic modes (A. Guaus)
- Some non-linear results (D. Biau & S. Brogniez)
- Related work on fluid-structure interactions:
  - ciliated propulsion (A. Dauptain & J. Favier)
  - flapping wing aerodynamics (J. Guerrero & H. Soueid)

SIGNIFICANCE OF THE SUBJECT

Hydro- and aero-elastic interactions are very important in a variety of disciplines, from aeronautics to civil engineering to bio-fluid-dynamics

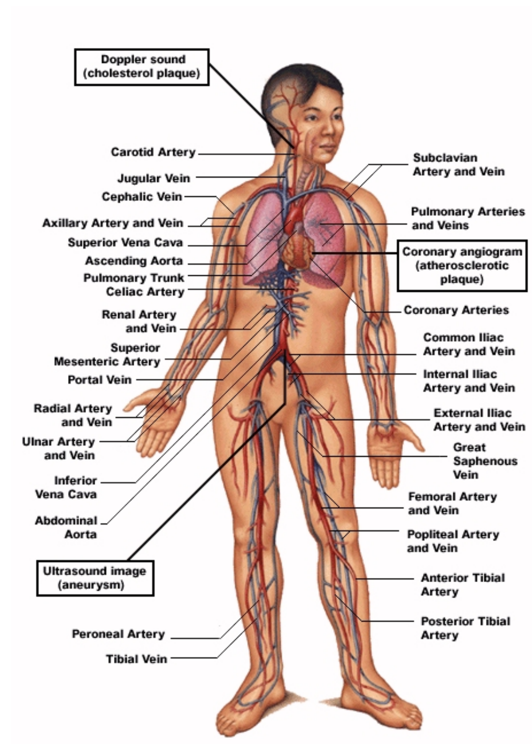

PREVIOUS WORK ON LINEAR STABILITY OF FLOWS OVER COMPLIANT WALLS

- J. Gray (1936), observation of swimming dolphins
- M.O. Kramer (1957), transition delay (?)
- T.B. Benjamin (1960) and M.T. Landahl (1962)
  SURFACE-BASED MODEL
- P.W. Carpenter (1985) with his group at the U. of Warwick
  - Coupling of the hydrodynamics with thin plate equations supported by springs and dampers
  - Effect of compliant walls on Tollmien-Schlichting waves, cross-flow vortices, streaks in boundary layers
  - Study of the hydroelastic instabilities (TWF, SD + coalescing modes)
- Y.S. Yeo (1985), U. of Cambridge, now at the National U. of Singapore
  VOLUME-BASED MODEL
  - Full coupling between the Navier equations for the solid and the flow
  - Anisotropic and multilayered materials
- M. Gad-el-Hak (1986)
  Experiments on a turbulent boundary layer, coating made of household gelatin or PVC plastisol, highlight the importance of static divergence waves

DEAN AND TAYLOR VORTEX FLOWS: THE FLUID MODEL

$$x = \frac{2\theta}{\gamma}, \quad y = \frac{2(r-R)}{\gamma R}, \quad z = \frac{2\xi}{\gamma R}$$

$$\gamma = 2h/R$$

$$\gamma \ll 1$$

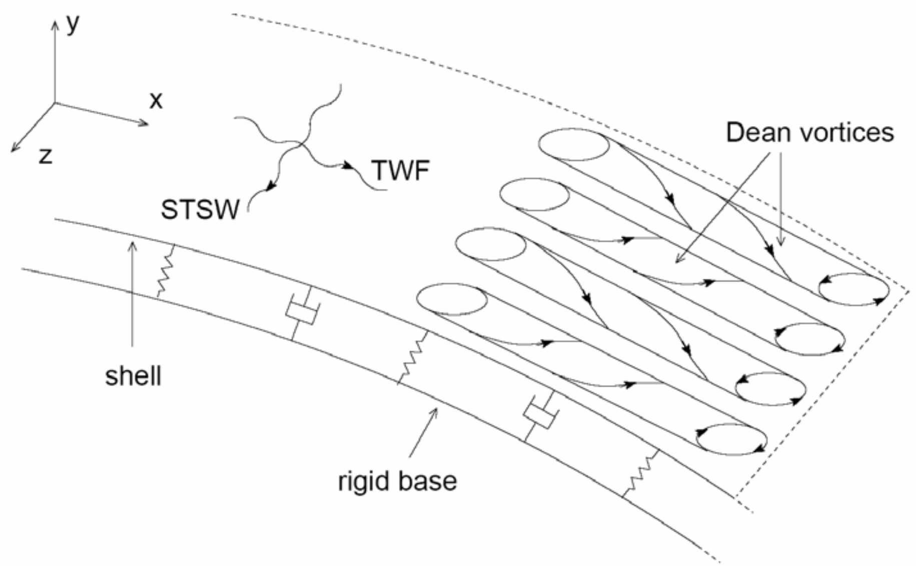

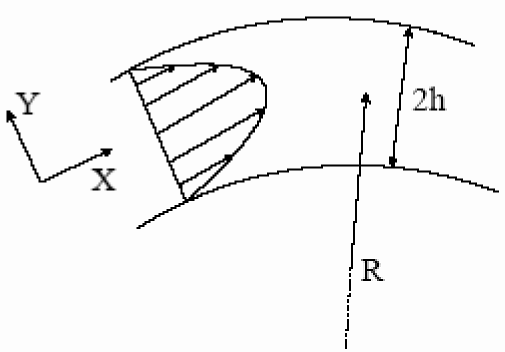

Figure 1. Sketch of the problem under investigation with some of the instability modes which can emerge: Dean vortices, travelling-wave flutter (TWF) and spanwise-travelling surface wave (STWF). The upper wall is not shown. Both walls are modeled as thin elastic shells supported by rigid frames through arrays of springs and dampers.

DEAN AND TAYLOR VORTEX FLOWS: THE FLUID MODEL

$$u = \frac{u_\theta}{U_0}, \quad v = \frac{u_r}{U_0}, \quad w = \frac{u_z}{U_0}, \quad p = \frac{p^*}{\rho U_0^2}, \quad t = \frac{U_0}{h} t^*$$

U_0 is the centerline velocity in one case, and ωR in the other

Base flow, CCPF: $U = (1 - y^2)(1 - \frac{1}{3}\gamma y)$

Base flow, Couette: $U(y) = \frac{1-y}{2} + \frac{\gamma}{2}\left(\frac{y^2}{4} + \frac{y}{2} - \frac{3}{4}\right)$

Disturbance equations to first order in γ: $\boxed{\hat{u}(y),\ \hat{v}(y),\ \hat{w}(y),\ \hat{p}(y)\ )e^{i\alpha x + i\beta z + \sigma t}}$

$$\begin{cases}
i\alpha\hat{u} + D\hat{v} + i\beta\hat{w} + \frac{\gamma}{2}\hat{v} - i\alpha\frac{\gamma}{2}y\hat{u} = 0, \\
\sigma\hat{u} + i\alpha\left(1 - \frac{\gamma y}{2}\right)U\hat{u} + U'\hat{v} + \frac{\gamma}{2}U\hat{v} = -i\alpha\left(1 - \frac{\gamma y}{2}\right)\hat{p} + \frac{1}{Re}(D^2 - k^2)\hat{u} \\
\qquad + \frac{\gamma}{Re}\left[\left(\frac{1}{2}D + y\alpha^2\right)\hat{u} + i\alpha\hat{v}\right] \\
\sigma\hat{v} + i\alpha\left(1 - \frac{\gamma y}{2}\right)U\hat{v} - \gamma U\hat{u} = -D\hat{p} + \frac{1}{Re}(D^2 - k^2)\hat{v} + \frac{\gamma}{Re}\left[\left(\frac{1}{2}D + y\alpha^2\right)\hat{v} - i\alpha\hat{u}\right] \\
\sigma\hat{w} + i\alpha\left(1 - \frac{\gamma y}{2}\right)U\hat{w} = -i\beta\hat{p} + \frac{1}{Re}(D^2 - k^2)\hat{w} + \frac{\gamma}{Re}\left(\frac{1}{2}D\hat{w} + y\alpha^2\right)\hat{w},
\end{cases}$$

DEAN AND TAYLOR VORTEX FLOWS: THE FLUID MODEL

Parameters: γ and $Re = U_0\, h/\nu$

α, β wavenumbers ($D = d/dy$)

σ growth rate of the instability

In the Dean (Taylor-Couette) problem the Dean (Taylor) number is normally used:

$$\begin{cases} De = Re\ \gamma^{1/2} \\ Ta = Re\ \gamma^{1/2} \end{cases}$$

LOVE’S CYLINDRICAL SHELL THEORY: THE WALL MODEL

$$\left[\left(m^* \frac{\partial^2}{\partial {t^*}^2} + d^* \frac{\partial}{\partial t^*} + B^* \Delta_h^2 - T^* \Delta_h + K^*\right)\Delta_h + \frac{E^* H}{R^2}\frac{\partial^4}{\partial {z^*}^4}\right]\eta^* = \begin{cases} \Delta_h p^*(h) \\ -\Delta_h p^*(-h) \end{cases}$$

where $\Delta_h = \frac{\partial^*}{\partial {x^*}^2} + \frac{\partial^2}{\partial {z^*}^2}$. In the equation above, m^* is the plate mass per unit area, d^* is the wall damping coefficient, $B^* = \frac{E^* H^3}{12(1-{\nu^*}^2)}$ is the flexural rigidity of the shell, with E^* Young modulus, H the thickness of the shell and ν^* Poisson’s ratio; K^* is the spring stiffness and T^* is the longitudinal tension per unit width.

Scaling of wall properties ensure that as *Re* (*i.e.* U_0) varies the same wall is considered:

$$m = \frac{m^*}{\rho h}, \quad d = \frac{d^* h}{\rho \nu}, \quad B = \frac{B^*}{\rho \nu^2 h}, \quad E = \frac{E^* h^2}{\rho \nu^2}, \quad K = \frac{K^* h^3}{\rho \nu^2}, \quad T = \frac{T^* h}{\rho \nu^2}$$

After writing the wall displacement, scaled by h, as a normal mode in the form $\eta = \hat{\eta}\, e^{\mathrm{i}\alpha x + \mathrm{i}\beta z + \sigma t}$, the following dimensionless shell equation is found:

$$\left[m\sigma^2 + \frac{d}{Re}\sigma + \frac{1}{Re^2}\left(Bk^4 + Tk^2 + K + \cancel{\frac{H}{h}\frac{\gamma^2}{2} E \frac{\beta^2}{k^2}}\right)\right]\hat{\eta} = \begin{cases} \hat{p}(1) \\ -\hat{p}(-1) \end{cases} \qquad (2.8)$$

LOVE'S CYLINDRICAL SHELL THEORY: THE WALL MODEL

The no-slip condition on the upper wall at $y = 1 + \eta$ reads:

$$U + u = 0, \quad v = \partial\eta/\partial t, \quad w = 0. \tag{2.9}$$

Linearising around $y = 1$ we find:

$$\hat{u} \; + \; \hat{\eta}\, U' = 0, \tag{2.10}$$

$$\hat{v} - \sigma\, \hat{\eta} = 0, \tag{2.11}$$

$$\hat{w} = 0, \tag{2.12}$$

and combining (2.10) and (2.11) allows to eliminate $\hat{\eta}$:

$$\sigma\hat{u} + U'\hat{v} = 0. \tag{2.13}$$

Likewise, introducing (2.10) and (2.11) into (2.8) yields:

$$m\sigma\hat{v} + \frac{1}{Re} d\hat{v} - \frac{1}{U' Re^2}\left(Bk^4 + K + Tk^2\right)\hat{u} = \hat{p}. \tag{2.14}$$

$m = 2,\ T = 0$ (following Davies and Carpenter), $\gamma = 0.025$ for the Dean problem (as in the experiments by Matsson & Alfredsson 1990), and $\gamma = 0.0174$ for the Taylor-Couette problem (as in the experiments by Prigent & Dauchot, 2000).

LINEAR STABILITY: HYDROELASTIC AND HYDRODYNAMIC MODES

$\alpha = 0$: streamwise invariant modes in curved channel

A new spanwise-travelling surface wave (STSW) appears and dominates in the long-wave limit

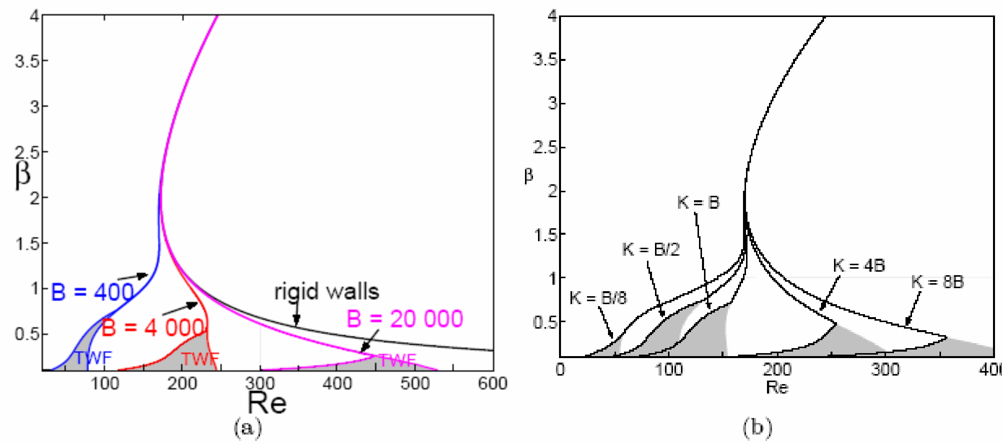

Figure 2. Neutral curves showing the effect of wall compliance on streamwise homogeneous disturbances. The grey regions correspond to an unstable spanwise travelling mode. The damping coefficient d is taken equal to zero. (a) $K = B/4$; vertical dashed lines are drawn for $Re = 225$ and $Re = 275$. (b) $B = 400$, effect of varying K.

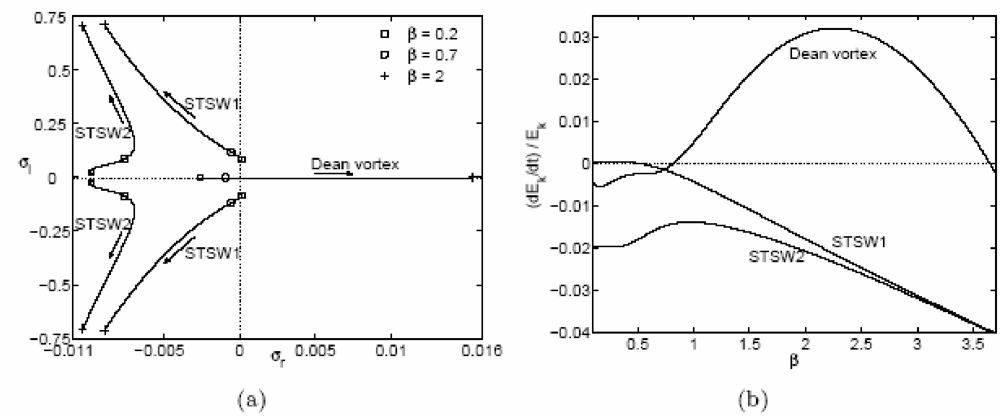

Figure 3. (a) Eigenvalue spectrum showing the evolution of the main streamwise homogeneous eigenmodes with the spanwise wavenumber ($0.1 \leq \beta \leq 2$) and (b) disturbance kinetic energy versus spanwise wavenumber ($0.1 \leq \beta \leq 3.7$) for the same modes. Arrows denote increasing β. The parameters are $Re = 225$, $K = 1000$, $B = 4000$ and $d = 0$.

Reynolds-Orr energy equation:

$$\frac{\mathrm{d}}{\mathrm{d}t}\int_{-1}^{1}\frac{1}{2}\overline{u_iu_i}\,\mathrm{d}y = \overbrace{-\int_{-1}^{1}U'\overline{uv}\,\mathrm{d}y}^{(I1)}\;\overbrace{-\frac{1}{Re}\int_{-1}^{1}\overline{\frac{\partial u_i}{\partial x_j}\frac{\partial u_i}{\partial x_j}}\,\mathrm{d}y}^{(I2)}$$

$$+\underbrace{\frac{\gamma}{2}\int_{-1}^{1}U\overline{uv}\,\mathrm{d}y}_{(G1)}\;\underbrace{\cancel{-\frac{\gamma}{2}\int_{-1}^{1}\overline{pv}\,\mathrm{d}y}}_{(G2)}+\underbrace{\cancel{\frac{\gamma}{Re}\int_{-1}^{1}\left(y\overline{\frac{\partial u_i}{\partial x}\frac{\partial u_i}{\partial x}}+\overline{u\frac{\partial v}{\partial x}}-\overline{v\frac{\partial u}{\partial x}}\right)\mathrm{d}y}}_{(G3)}$$

$$\underbrace{-\overline{vp}\Big|_{-1}^{1}}_{(C1)}+\underbrace{\frac{1}{Re}\left(\overline{u\frac{\partial u}{\partial y}}+\overline{v\frac{\partial v}{\partial y}}\right)\Big|_{-1}^{1}}_{(C2)}+\underbrace{\cancel{\frac{\gamma}{4Re}\left(\overline{u^2}+\overline{v^2}\right)\Big|_{-1}^{1}}}_{(C3)}.$$

centrifugal energy production term

irreversible work done on the wall by p

energy source/sink term (only sink in the case of TS waves)

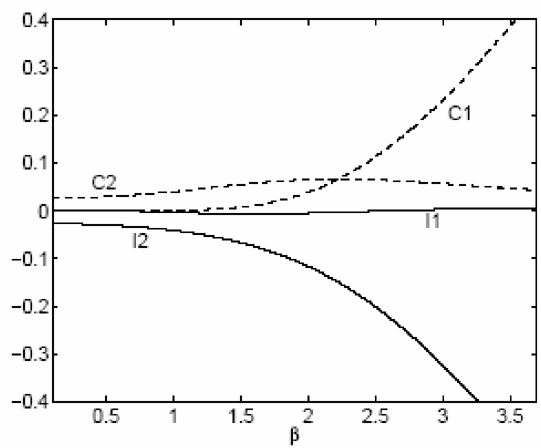

Figure 4. Main terms in the disturbance energy balance, normalized by E_k for the STSW1 mode; same parameters as in figure 3(b).

LINEAR STABILITY: HYDROELASTIC AND HYDRODYNAMIC MODES

Reynolds-Orr energy equation:

$$
\frac{\mathrm{d}}{\mathrm{d}t}\int_{-1}^{1}\frac{1}{2}\overline{u_i u_i}\,\mathrm{d}y = \overbrace{-\int_{-1}^{1}U'\overline{uv}\,\mathrm{d}y}^{(I1)}\;\overbrace{-\frac{1}{Re}\int_{-1}^{1}\overline{\frac{\partial u_i}{\partial x_j}\frac{\partial u_i}{\partial x_j}}\,\mathrm{d}y}^{(I2)}
$$

$$
\underbrace{+\frac{\gamma}{2}\int_{-1}^{1}U\overline{uv}\,\mathrm{d}y}_{(G1)}\;\underbrace{\cancel{-\frac{\gamma}{2}\int_{-1}^{1}\overline{pv}\,\mathrm{d}y}}_{(G2)}\;\underbrace{\cancel{+\frac{\gamma}{Re}\int_{-1}^{1}\left(y\overline{\frac{\partial u_i}{\partial x}\frac{\partial u_i}{\partial x}}+\overline{u\frac{\partial v}{\partial x}}-\overline{v\frac{\partial u}{\partial x}}\right)\mathrm{d}y}}_{(G3)}
$$

centrifugal energy production term

$$
\underbrace{-\overline{vp}\Big|_{-1}^{1}}_{(C1)}\;\underbrace{+\frac{1}{Re}\left(\overline{u\frac{\partial u}{\partial y}}+\overline{v\frac{\partial v}{\partial y}}\right)\Big|_{-1}^{1}}_{(C2)}\;\underbrace{\cancel{+\frac{\gamma}{4Re}\left(\overline{u^2}+\overline{v^2}\right)\Big|_{-1}^{1}}}_{(C3)}.
$$

energy source/sink term (only sink in the case of TS waves)

irreversible work done on the wall by p

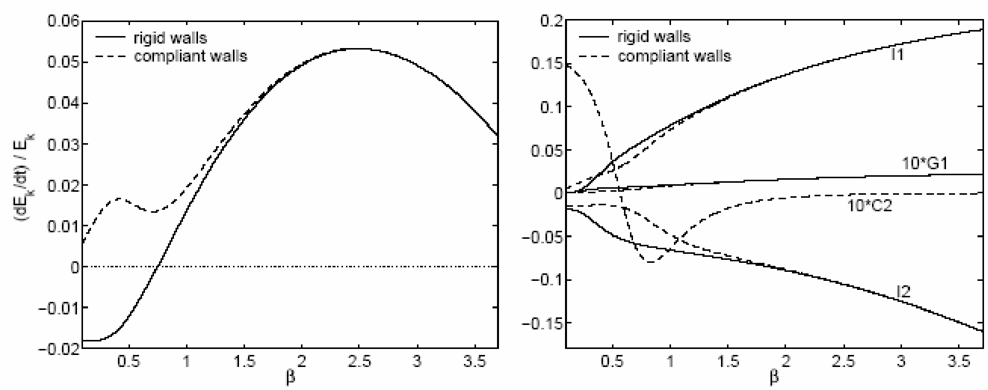

(a) (b)

Figure 5. (a) Disturbance energy growth rate versus spanwise wavenumber and (b) main terms in the disturbance energy balance for the Dean vortex mode. All terms are normalized by E_k. The parameters are $Re = 275$, $K = 1000$, $B = 4000$ and $d = 0$.

LINEAR STABILITY: HYDROELASTIC AND HYDRODYNAMIC MODES

Mode shapes

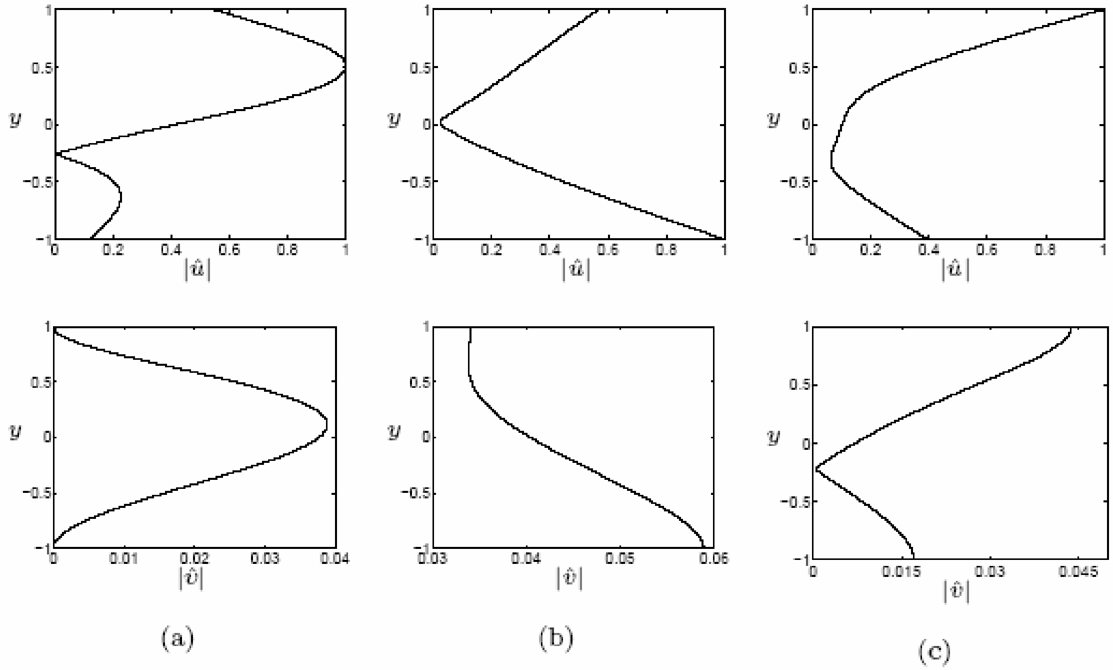

Figure 6. Longitudinal $\hat{u}$ and wall normal $\hat{v}$ velocities (absolute values normalised by $\hat{u}$ maximum) for the case shown in figure 3(a) with $\beta = 0.7$. (a) stable Dean vortex, (b) stable STSW1, (c) stable STSW2.

LINEAR STABILITY: HYDROELASTIC AND HYDRODYNAMIC MODES

Effect of damping coefficient

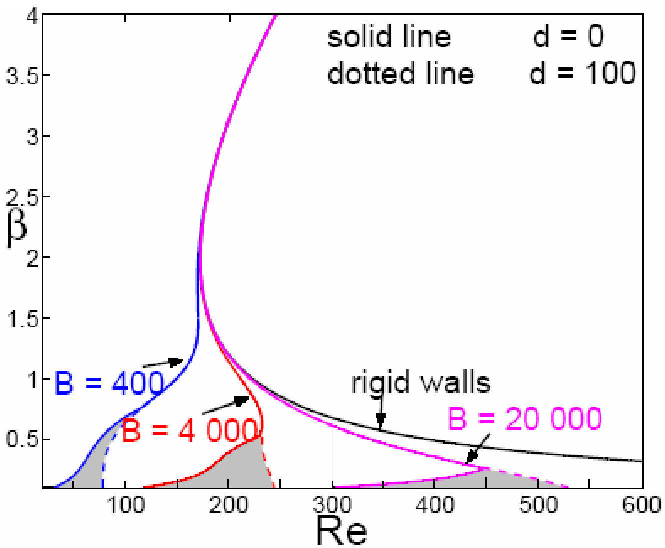

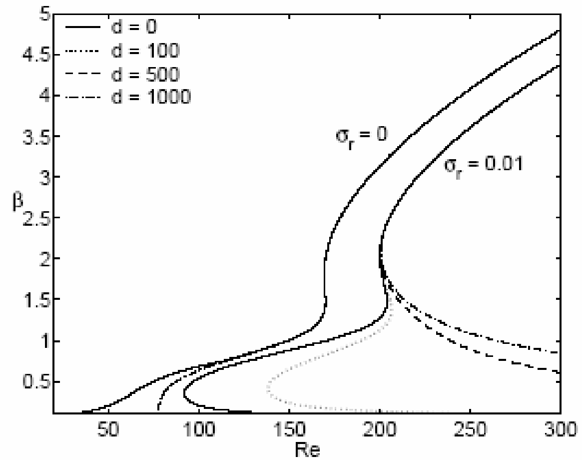

Figure 7. Neutral curves and curves of constant growth rate ($\sigma_r = 0.01$) for different damping coefficients. The parameters are $K = 100$ and $B = 400$.

LINEAR STABILITY: HYDROELASTIC AND HYDRODYNAMIC MODES

β = 0: TS-like mode
in curved channel

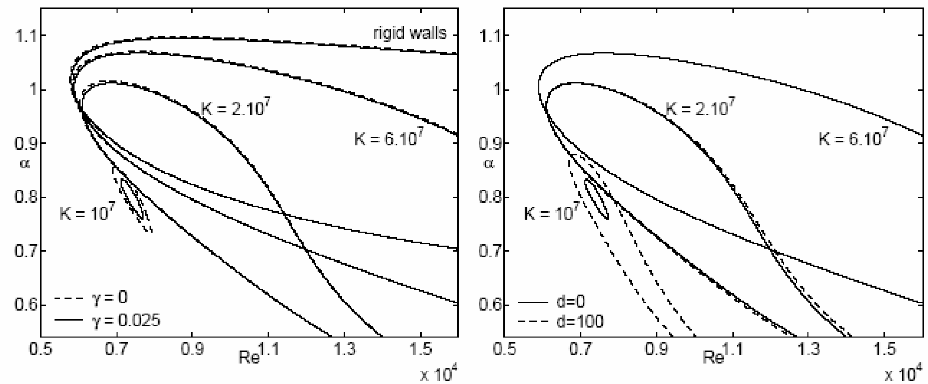

(a) (b)

Figure 8. Neutral curves for the Tollmien-Schlichting instability showing the effect of (a) wall compliance and wall curvature for $d = 0$ and (b) wall damping for $\gamma = 0.025$. In both cases we have $B = 4K$.

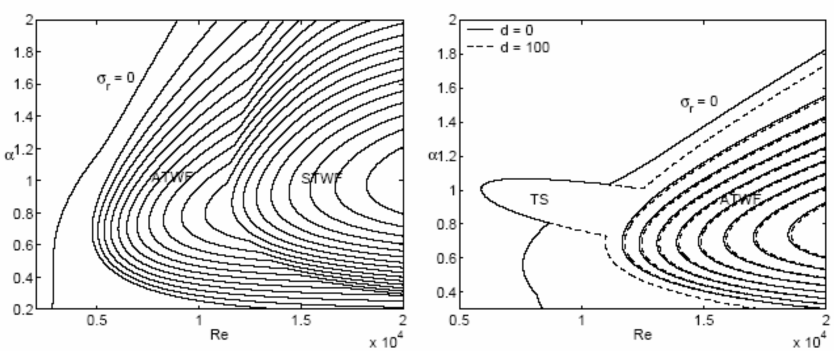

(a) (b)

Figure 11. Curves of constant positive growth rate (lines are equally spaced of $\Delta\sigma_r = 0.01$) for spanwise homogeneous disturbances showing the dominant modes with (a) $K = 10^7$, $B = 4 \times 10^7$ and (b) $K = 6 \times 10^7$, $B = 24 \times 10^7$. In (b) the effect of wall damping is also shown.

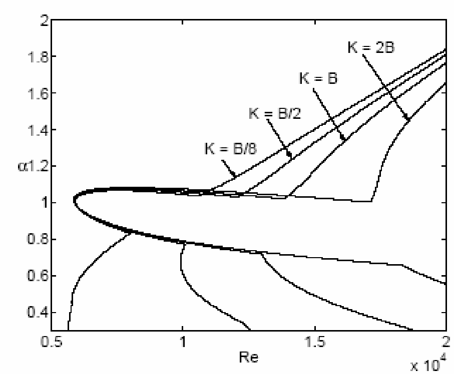

Figure 12. Neutral curves showing the influence of the spring stiffness on streamwise homogeneous disturbances for a fixed flexural rigidity $B = 24 \times 10^7$ with $d = 0$.

LINEAR STABILITY: HYDROELASTIC AND HYDRODYNAMIC MODES

Disturbances in the Couette system $\boxed{\alpha = n\gamma/2}$

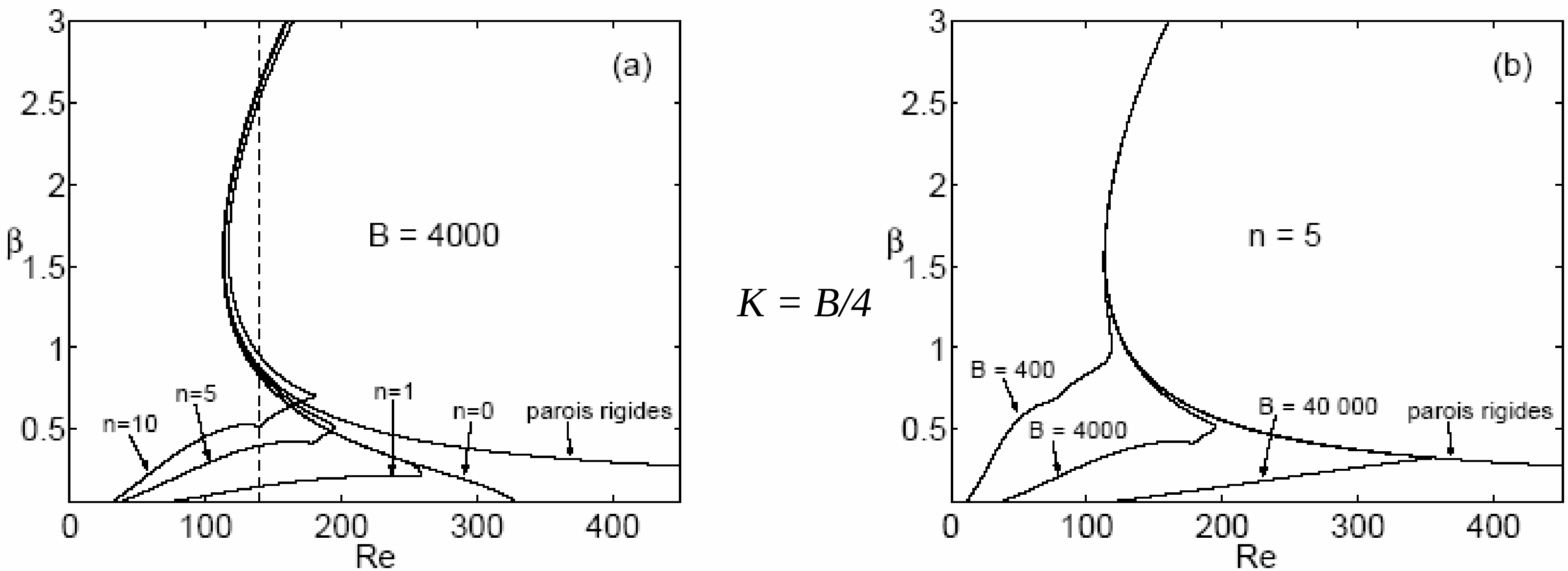

FIG. 1 – (a) Courbes neutres pour différents nombres d'onde azimutaux $\alpha = n\gamma/2$ pour des parois compliantes de paramètres $B = 4000$, $d = 0$. En pointillé : $Re = 140$. (b) Courbes neutres montrant l'influence de la flexibilité des parois pour $n = 5$ avec $d = 0$.

LINEAR STABILITY: HYDROELASTIC AND HYDRODYNAMIC MODES

Disturbances in the Couette system

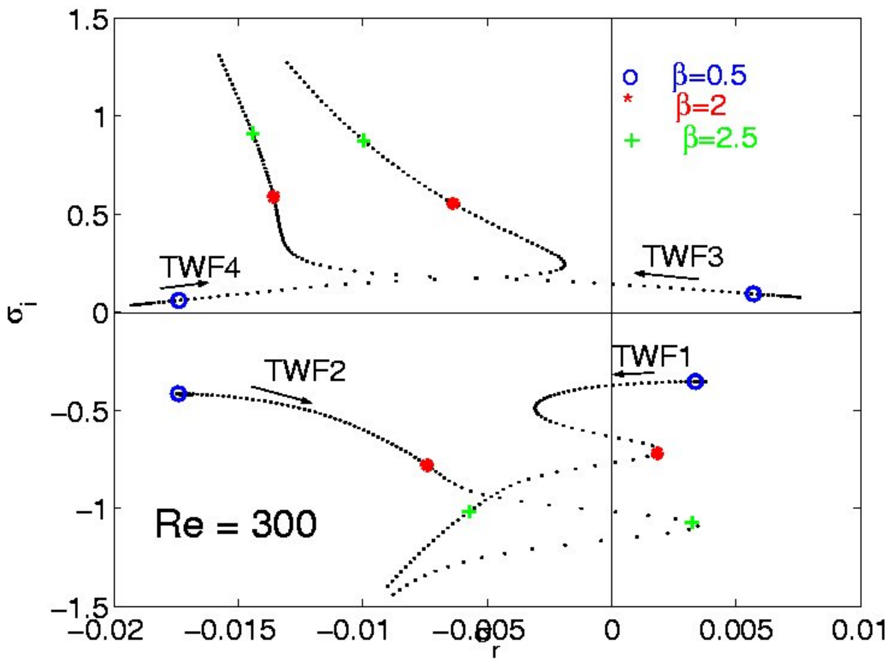

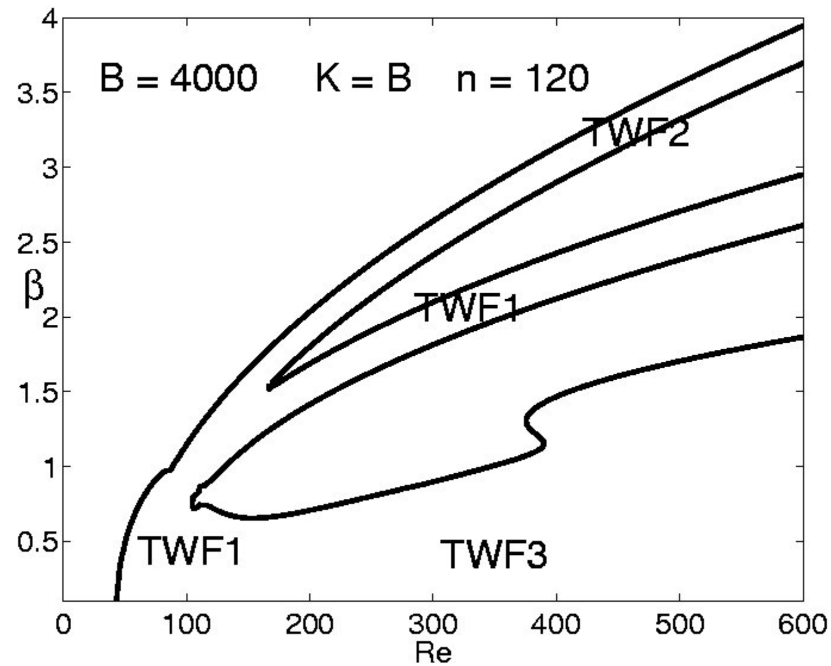

LINEAR STABILITY: HYDROELASTIC AND HYDRODYNAMIC MODES

Disturbances in the Couette system

B = 4000: an optimal azimuthal wavenumber n exists which minimizes Re_c for each B and K. For example,

$K = B/16$:	$n_{opt} = 35$	λ_θ = 20.63 h
$K = 8B$:	$n_{opt} = 131$	λ_θ = 5.5 h

This implies that for increasing $\alpha_w = (K/B)^{1/4}$ (wavenumber at which free waves in the compliant wall propagate at minimum possible phase speed) the azimuthally travelling waves shorten (coherent with the TWF case of the curved channel flow).

SOME NON-LINEAR RESULTS

wall model:

$$C_0\frac{\partial^2\eta}{\partial t^2}+C_1\frac{\partial\eta}{\partial t}+C_2\left(\frac{\partial^4\eta}{\partial x_1^4}+\frac{\partial^4\eta}{\partial x_3^4}+2\frac{\partial^4\eta}{\partial x_1^2x_3^2}\right)+C_3\eta-C_x\frac{\partial^2\eta}{\partial x_1^2}-C_z\frac{\partial^2\eta}{\partial x_3^2}=-p_w,$$

the coefficients are:

$C_0 = 2 \times 10^3$ plate density
$C_1 = 10^3$ wall damping
$C_2 = 0$ flexural rigidity
$C_3 = 10^4$ spring stiffness
$C_x = C_z = 0$ tension
p_w = wall pressure given by the fluid solver

fluid model:
Navier-Stokes equations for Taylor-Couette flow (narrow gap hypothesis)
Taylor number: $Ta = 3000$

SOME NON-LINEAR RESULTS

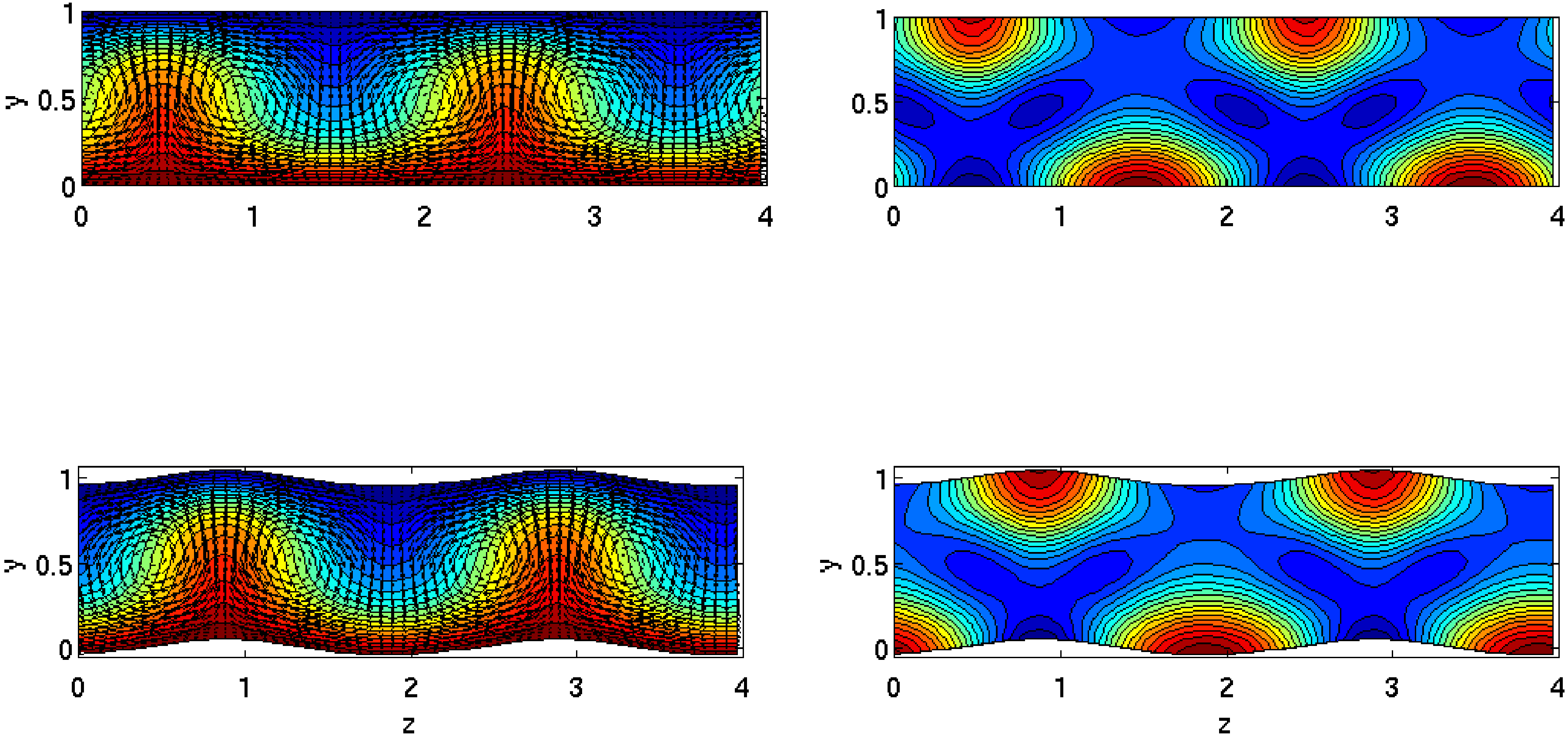

RELATED WORK ON FLUID-STRUCTURE INTERACTIONS: CILIATED PROPULSION

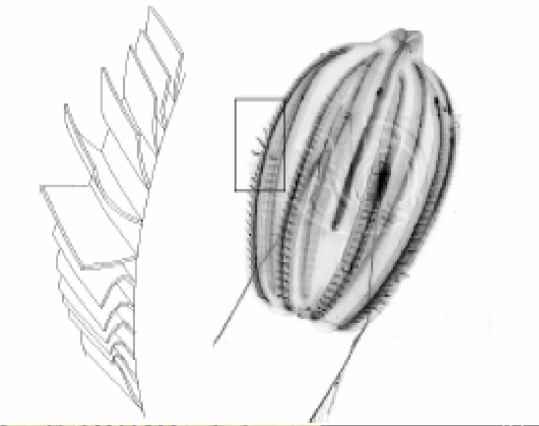

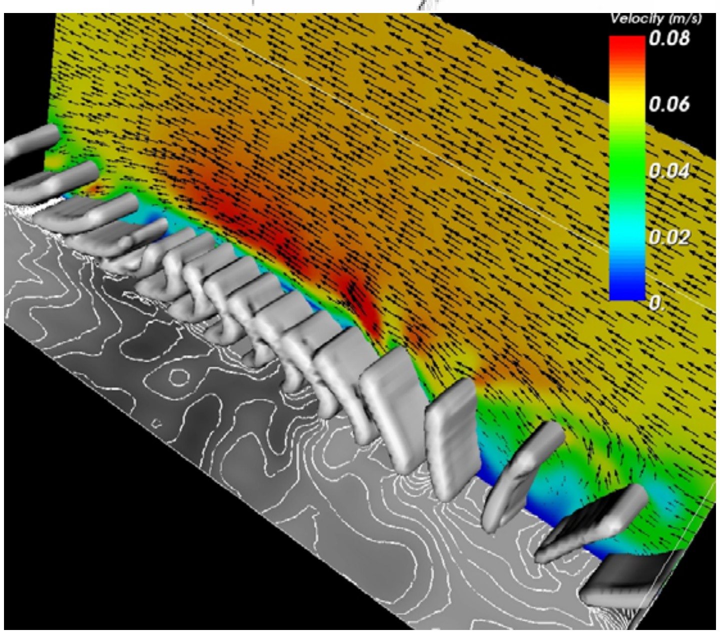

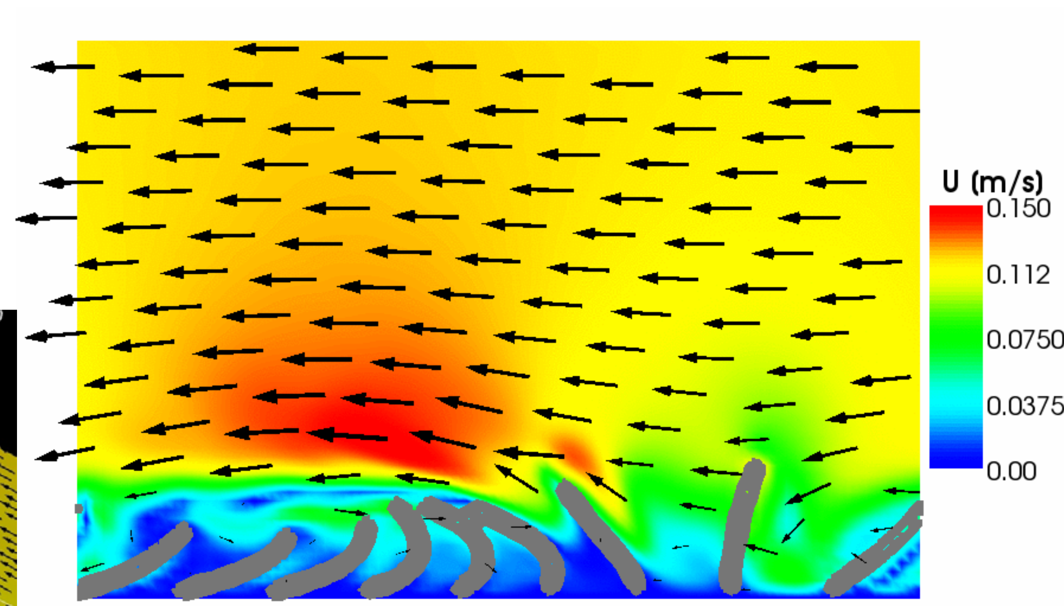

RELATED WORK ON FLUID-STRUCTURE INTERACTIONS: FLAPPING WING AERODYNAMICS